Two Toc34 Homologues with Different Properties†

Marko Jelic, Jürgen Soll, and Enrico Schleiff*

LMU München, Menzinger Strasse 67, 80638 München, Germany

Received January 2, 2003; Revised Manuscript Received March 26, 2003

ABSTRACT: The Toc34 isoforms are located in the outer envelope membrane of plastids. In pea, Toc34 functions as a GTP dependent receptor for preproteins, which is controlled by protein phosphorylation. Two members of this family are present in *Arabidopsis thaliana*, namely, atToc34 and atToc33. AtToc33 is phosphorylated, as is the homologue in *P. sativum*, while atToc34 is not. The phosphorylation of atToc33 occurs on serine 181. The highest affinity for dimerization was for the heterodimer between Toc33 and Toc34 in the absence of GTP or GDP. Both proteins, atToc33 and atToc34, bind GTP with significantly higher affinity than GDP and are able to hydrolyze GTP. The intrinsic GTP hydrolysis rate of both proteins is comparable. Hydrolysis is strongly stimulated in the presence of preproteins, which are in turn released upon GTP hydrolysis. Preprotein subclasses exist, which show a strong preference for either the atToc33 or the atToc34 receptor as revealed by GTP hydrolysis rate stimulation and receptor precursor dissociation constants. Detailed analysis of precursor recognition supports the model of a GTP hydrolysis regulated receptor ligand interaction.

Translocation of proteins across membranes is facilitated by proteinaceous translocation machineries (*1*−*3*). These translocation systems are comprised of receptor proteins and translocation channels. Protein translocation across the outer envelope of chloroplasts is achieved by the Toc complex (Translocon of the outer envelope of chloroplasts). At least four proteins at the outer envelope are involved in the translocation, namely, the two GTPase type receptor proteins Toc159 and Toc34 (*4*−*6*), the translocation channel Toc75 (*7*, *8*), and Toc64, which is yet to be functionally characterized (*9*). Further, the accessibility of the complete genome of *Arabidopsis thaliana* revealed several isoforms of each of the components (*10*). For example, four isoforms of the Toc159 receptor exist, namely, Toc159, Toc132, Toc120, and Toc90 (*11*, *12*). For Toc34, two isoforms named Toc34 and Toc33 were identified (*13*, *14*). However, little is known regarding the distinct functional and regulatory properties of the different isoforms. Current results suggest that Toc159 is essential for chloroplast biogenesis (*11*), indicating that its function cannot be performed by the other isoforms. The knock out of Toc33 in *A. thaliana* showed a similar phenotype again suggesting that atToc34 cannot completely complement the function of atToc33 (*13*). In contrast, the atToc34 knock out did not show such a drastic phenotype (*14*). This observation lead to the hypothesis that both proteins are either required for a different subset of proteins (*11*, *13*) or that they might be differentially regulated and expressed. Indeed, Northern blot analysis revealed a different transcript distribution of the two isoforms. Whereas Toc34 was mainly identified in stems, flowers, and roots, Toc33 existed in all tissues (*14*). Furthermore, it could be demonstrated that plastids from roots of the atToc33 and atToc159 knock out plants became photosynthetically active after prolonged light treatment demonstrating the ability of these plastids to import proteins involved in photosynthesis (*15*). However, it still remains to be investigated whether all isoforms of one protein class are similarly regulated and if they reveal similar affinities for all incoming preproteins.

From previous studies on Toc34 from *P. sativum*, a scheme of action for this GTPase type receptor was proposed. The receptor Toc34 can be phosphorylated in vitro (*16*) and in vivo (*17*) by a kinase localized in the outer envelope of chloroplasts (*18*, *19*). This phosphorylation inhibits GTP binding and as a consequence abolishes interaction with the precursor form of the small subunit of RUBISCO (preSSU)[1] (*16*) suggesting that phosphorylation functions as an on/off switch for receptor function. The nonphosphorylated receptor recognizes the incoming preprotein with highest affinity when loaded with GTP (*16*, *20*, *21*). Addition of a C-terminal truncated form of atToc33 to a precursor protein population prior to addition of chloroplasts reduces the binding of preSSU to the surface of the organelle in a GTP dependent manner in vitro (*14*), corroborating the receptor function of atToc33/Toc34. Indeed, it was demonstrated in a reconstituted system that Toc34 from *P. sativum* interacts directly with preSSU (*16*, *21*). This interaction leads to an increase of GTP hydrolysis (*17*) leading to the release of the preprotein because the affinity of the precursor for the GDP loaded receptor is significantly lower than for the GTP form

† This work was supported by the Deutsche Forschungsgesellschaft.

* Corresponding author. Phone: 0049-89-17861-182. Fax: 0049-89-17861-185. E-mail: schleiff@botanik.biologie.uni-muenchen.de.

[1] Abbreviations: APC, γ subunit of the chloroplast ATP synthetase; at, *Arabidopsis thaliana*; CAO, chlorophyll *a* oxygenase; FNR, ferredoxin: $NADP^+$ oxidoreductase; GAP, GTPase activating protein; GEF, GTP/GDP exchange factor; HCF136, high chlorophyll fluorescence phenotype protein 136; mSSU, mature form of SSU; preAPC/preCAO/preFNR/preHCF136/preSSU, preprotein form of APC/CAO/FNR/HCF136/SSU; preOE23/33, preprotein form of 23/33 kDa subunit of the oxygen evolving complex; ps, Pisum sativum; SSU, small subunit of ribulose 1,5-bisphosphate carboxylase-oxygenase (rubisco); Tic/Toc, translocon of the outer/inner envelope of chloroplast; Toc33/34ΔTM, cytosolic domain of the 33/34 kDa subunit of the Toc complex.

10.1021/bi034001q CCC: $25.00
Published on Web 04/23/2003

(*21*). This is in line with the in situ observation that the association between Toc34 and preprotein can only be observed in the absence of GTP since addition of GTP will induce hydrolysis and subsequently the release of the preprotein from the receptor (*20*, *22*).

Recent data on structural features of Toc34 demonstrated that this protein belongs to classical GTPase proteins (*21*). Further statistical analysis of the sequence of Toc34 indicated that Toc34, together with the G-domain of Toc159, belongs to the septine subfamily, which is characterized by the loss of the asparagine within the NKxD motif (*23*) of GTP binding domains (*24*, *25*). Interestingly, the only further members of this subgroup belong to the AIG1 family (avrRpt2-induced gene 1). AIG1 is a protein induced in *A. thaliana* in response to bacterial pathogens (*26*). The crystal structure of psToc34 further underlines this statistical observation (*27*) and further supports the observation that phosphorylation on serine 113 of psToc34 (*17*) influences the GTP binding of the receptor protein since serine 113 is located in the switch 1 domain essential for GTP hydrolysis.

Here, we wanted to study the atToc33/Toc34 receptor proteins to understand the differential function of these proteins. We present evidence for a cycle of GTP hydrolysis regulated association and dissociation of preproteins from the receptor. Furthermore, we can demonstrate differential substrate specificity of the two receptor proteins. In addition, both receptors are regulated by different mechanisms. The analysis of the phosphorylation site of Toc33 revealed a specific amino acid motif, which might be used to identify the homologues of Toc33 and Toc34 in different plant species.

MATERIALS AND METHODS

Materials. The bacterial strains BL21-DE3 and NovaBlue (DE3) were obtained from Stratagene (Madison, WI), and the vectors pET21d and pET23d were from Novagen (La Jolla, CA). [γ^{32}P]-ATP (3000 Ci/mmol) and [α^{32}P]-GTP (3000 Ci/mmol) were purchased from Amersham Pharmacia Biotech. (Freiburg, Germany). All other chemicals used were obtained from Roth (Karlsruhe, Germany) or Sigma (Munich, Germany). Standard procedures such as the purification of outer envelopes of chloroplasts or SDS−PAGE are described elsewhere (*6*, *16*).

Generation, Mutagenesis, and Expression of the Preproteins atToc33ΔTM and atToc34ΔTM. Point mutations were introduced by standard polymerase chain reaction using the cDNA encoding for atToc34 and atToc33 as template. The encoding DNA was cloned into pET21d. Point mutations were confirmed by sequencing, and constructs were expressed and purified as previously described (*16*). The cDNA encoding preHCF136, preAPC, preFNR, and preCAO were amplified by PCR and cloned into pET21d. Cloning and point mutations were confirmed by sequencing. Proteins were expressed and purified as previously described using Talon chelated chromatography (*17*, *21*, *28*). Inclusion bodies were solubilized in 25 mM Hepes pH 7.6, 8 M urea, 50 mM DTT. After purification, Toc33/34ΔTM and mutants were dialyzed into the buffer used for the experiments.

Immobilization of Toc33 onto GTP or preSSU Affinity Matrix. 0.1 μM purified and phosphorylated Toc33ΔTM in buffer A (20 mM Tricine, pH 7.6, 50 mM NaCl, 1 mM $MgCl_2$, 1 mM DTT) was incubated with GTP or GDP agarose (1 mM immobilized nucleotide final) for 10 min at room temperature. After incubation, the agarose was washed three times with 50 volumes of buffer A, and remaining Toc33ΔTM was eluted by adding SDS-sample buffer and boiling at 95 °C for 3 min. The specificity of the binding was controlled by addition of equal amounts of albumin, which did not bind to the column under the conditions used.

PreSSU and mSSU were coupled to Toyopearl (TosoHaas Biosep, Germany) by a method previously described elsewhere (*28*). The phosphorylated Toc33 protein was incubated for 5 min with the prepared affinity matrix in buffer A in the presence of 1 mM GMP-PNP. The affinity matrix was washed three times with 50 volumes of buffer A. The remaining sample was eluted by addition of SDS-sample buffer. All fractions were precipitated and subjected to SDS−PAGE analysis, immunoblotting, and autoradiography.

GTP Hydrolysis Assay. Indicated amounts of atToc34ΔTM or atToc33ΔTM were incubated in 10 μL of solution containing 20 mM Tricine/KOH, pH 7.6, 1 mM $MgCl_2$, 50 mM NaCl, 1 mM DTT with [α^{32}P]-GTP. Nucleotides were separated on PEI-cellulose plates (Merck, Darmstadt, Germany) using 600 mM NaH_2PO_4 at pH 3.4 as developing solvent. The hydrolysis of GTP was analyzed by the Michaelis−Menten equation

$$v_o = V_{max}[GTP]/([GTP] + K_m) \quad (1)$$

where v_o is the initial hydrolysis rate at a given GTP concentration, V_{max} is the maximal rate of hydrolysis, and K_m is the Michaelis−Menten constant. The catalytic constant k_{cat} was calculated by

$$k_{cat} = V_{max}/[Enzyme]_T \quad (2)$$

GTP Hydrolysis and preSSU Release. Per reaction, 0.1 nmol of atToc33 was coupled to an affinity matrix, and coupling efficiency was controlled by analysis of the flow through. The protein was incubated at 2 °C with 500 nmol of GTP containing [α^{32}P]-GTP. After 2 min, unbound GTP was removed by centrifugation of the affinity matrix at 2000*g* at 2 °C. The GTP loaded Toc33 was then incubated with 0.1 nmol [^{35}S]-preSSU for 2 min at 2 °C. Unbound preSSU was removed again by centrifugation. This mixture was shifted to room temperature for indicated times. The flow through was then analyzed for released preSSU using SDS−PAGE. For calibration, the loaded amount of preSSU was also subjected to SDS−PAGE. To assay the hydrolysis, the complete reaction mixture was separated on PEI-cellulose plates. For calibration, 0.1 nmol of GTP was also loaded. The reaction was controlled by the investigation of (i) the release of preSSU and GTP hydrolysis at 2 °C, (ii) the release of preSSU after binding to GMP-PNP loaded Toc33, and (iii) the hydrolysis of GTP by Toc33 in the absence of preSSU.

Phosphorylation and Phospho-amino Acid Analysis of atToc33 and atToc34. Toc34ΔTM and Toc33ΔTM were incubated for 10 min with outer envelope membranes and 10 or 50 nM [γ^{32}P]-ATP (3000 Ci/mmol) in 20 mM Tricine/KOH, pH 7.6, 10 μM ATP, 5 mM $MgCl_2$, 0.5 mM $MnCl_2$ at room temperature in 50 μL final volume. Proteins were

subjected to SDS−PAGE without further treatment, and phosphorylation was visualized by autoradiography. Phospho-amino acid analysis was performed as described earlier (*29*). In brief: phosphorylated Toc33ΔTM was hydrolyzed by 6 N HCl in the presence of unlabeled phospho-amino acids (phospho-tyrosine, phospho-threonine, phospho-serine, 20 μg each). The solvent was evaporated, and the residue was resuspended in water. The solution was spotted onto a precoated Silica thin-layer plate (Merck, Kieselgel 60), and amino acids were separated by 1000 V for 4 h using glacial acetic acid/formic acid/H_2O (78:25:897) as developing solvent. The phospho-amino acids were stained using ninhydrin, and radioactivity was detected by autoradiography.

Visualization and Quantification of the Hydrolysis or Phosphorylation. Phosphorylation or GTP hydrolysis of either Toc34ΔTM or Toc33ΔTM by radioactive labeled nucleotides was visualized or quantified by different methods. For visualization of radioactive probes, the gel or the DC plate was exposed to a X-OMAT-LS film (Kodak, Rochester, NY) or to a Phospho-Image plate (Fuji-Film, Tokyo, Japan). Data were transferred to Adope Photoshop 5.0 LE. For quantification, the Phospho-Image plate was scanned using a Phospho-Image Reader BAS 1500 (Fuji-Film, Tokyo, Japan) and quantified using an Aida-Image Analyzer (Raytest Isotopenmessgeräte GmbH, Staubenhard, Germany). Data were presented by using Sigma Plot 5.0 (SPSS Inc., Chicago, IL).

Activation of IAsys CMD Cuvette, Toc34, and Toc33 Coupling and Binding Experiments. The activation and coupling procedure was previously described in detail (*21*). In brief: each chamber of the carboxylmethyl-dextrane coated cuvette was incubated with 70 μL of HBST (10 mM Hepes/KOH pH 7.4, 138 mM NaCl, 2.7 mM KCl, 0.05% Tween 20) until a stable baseline was observed. Then, 100 μL of a fresh mixture containing 100 mM 1-ethyl-3-(3-dimethylaminopropyl) carbodiimide and 29 mM *N*-hydroxy-succinimide (EDC/NHS) was added. After 15 min, EDC/NHS was added a second time for 15 min. The buffer was then replaced by 33 μL of 100 mM NTA (Qiagen, Hilden, Germany), and cuvettes were incubated for 10 min. Both chambers were washed three times with HBST and then incubated for at least 1 min in the same buffer. Additional coupling sites were blocked for 2 min by addition of 100 μL of 1 M ethanolamine, pH 8.5. Nickel was loaded by incubation with 50 mM nickel sulfate in 10 mM Hepes/KOH pH 8.0 for 5 min. This step was repeated three times, followed by three wash steps with HBST. Both chambers were washed twice with 90 μL of PGIW buffer (50 mM sodium phosphate pH 6.8, 10% glycerol, 300 mM imidazole, 300 mM NaCl) followed by 3 min incubation in the same buffer.

Prior to use, His-tagged proteins were dialyzed for 16 h against 10 mM sodium phosphate pH 8, 50 mM NaCl, 5% glycerol, 0.7 mM β-mercaptoethanol, and 0.01% Triton X100. Proteins were diluted to a final concentration of 0.1 μg/μL with HBST, and 100 μL was incubated in each chamber until equilibrium was reached. Both chambers were washed with HBST and incubated until equilibrium was reached again. This procedure was repeated to yield between 0.5 and 15 nM (in 100 μL of reaction volume) coupled protein. Finally, both chambers were incubated with HBST until experiments were performed.

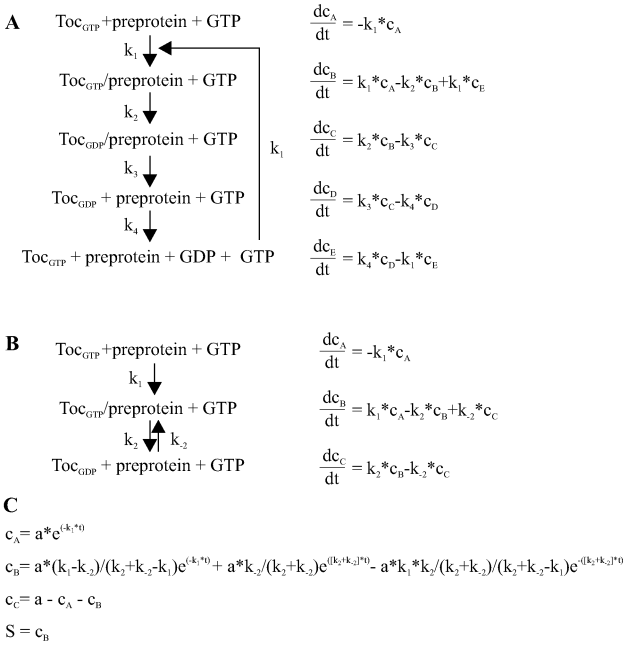

FIGURE 1: Reaction scheme for the preprotein recognition. (A) The exact reaction scheme for the Toc33/34—preprotein recognition is outlined. (B) A simplified reaction scheme is given. This model can be analytically described. (C) The solutions to the differential equations are shown. The signal (S) observed is only this of preprotein/Toc complexes. Therefore, the equation for the analysis is given.

For binding experiments, both chambers of the Ni-NTA cuvette were filled with 90 μL of the binding buffer (20 mM Hepes/KOH, pH 8.0, 50 mM NaCl, 0.05% Triton X100, 2.5% glycerol, and 0.01% fatty acid free BSA) and allowed to equilibrate. A new baseline was established, and binding was initiated by injection of 1−10 μL of the indicated amounts of proteins into their respective chambers as described in the figure legends. When binding was performed in the presence of GTP, 0.5 mM $MgCl_2$ was added. Dissociation was performed in 90 μL of the same buffer (except GTP). For surface regeneration between experiments, both chambers were extensively washed with 20 mM Hepes/KOH, pH 8.0, 150 mM NaCl, 0.1% Triton X100, 2.5% glycerol, and 0.01% BSA.

In some cases (Toc34ΔTM and for some experiments preSSU and preOE33), His-tagged proteins were used as ligand. The use of His-tagged ligands was possible for two reasons: first, the association of preSSU containing and not containing a His-tag with immobilized Toc34 was found to be identical (not shown). Second, for all measurements using a His-tagged ligand, self-immobilization could not be observed as controlled in the parallel cuvette (not shown).

Analysis and Quantification of IAsys Biosensor Binding Curves. Data files from IAsys plus were further analyzed using Sigma Plot 2000 (SPSS Inc.). Association was analyzed by nonlinear regression as previously described in detail (*21*), except for the binding of preproteins in the presence of GTP. This association was at least three-phasic. The process should be described as outlined in Figure 1A, but this type of reaction can only be numerically processed. However, the resolution of changes is limited by that technique used, meaning we cannot differentiate between Toc/GTP and Toc/GDP. Therefore, the analytically describable system can be limited by describing the first fast association reaction (Figure

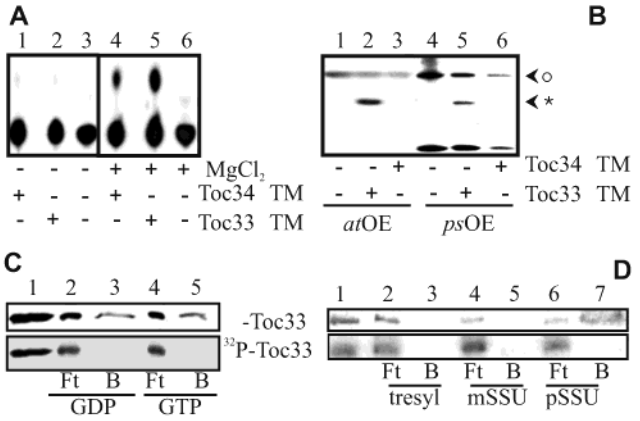

FIGURE 2: Receptor function of the GTPase atToc33, but not atToc34, is regulated by phosphorylation. (A) Hydrolysis of [α-^{32}P] GTP by 1 μg of heterologously expressed atToc34ΔTM (lanes 2, 4) or atToc33ΔTM (lanes 3, 5) was determined in the absence (lanes 1−3) or presence (lanes 4−6) of 1 mM $MgCl_2$. (B) Expressed atToc33ΔTM (lanes 2, 5) or atToc34ΔTM (lanes 3, 6) were incubated with outer envelope membranes from *A. thaliana* (lanes 1−3) or *P. sativum* (lanes 4−6) in the presence of [γ-^{32}P] ATP. The position of the endogenous psToc34 is indicated (○). (C) AtToc33ΔTM was incubated with outer envelope membranes *A. thaliana* in the presence of [γ-^{32}P] ATP. The phosphorylated protein (lane 1) was then incubated with GDP (lanes 2, 3) or GTP (lanes 4, 5) coated affinity matrix. The flow through (lanes 2, 4) and the bound protein (lanes 3, 5) were collected, subjected to SDS−PAGE, and immunodecorated with Toc33 antibodies. The Western blot (upper panel) and the autoradiogram (lower panel) are shown. (D) Phosphorylated atToc33ΔTM (lane 1) was incubated with tresyl affinity matrix (lanes 2, 3) coated with mSSU (lanes 4, 5) or preSSU (lanes 6, 7). The flow through (lanes 2, 4, 6) and the bound protein (lanes 3, 5, 7) were collected, subjected to SDS−PAGE, and immunodecorated with Toc33 antibodies. The Western blot (upper panel) and the autoradiogram (lower panel) are shown.

1B, step 1), the initial dissociation (Figure 1B, step 2), and reaching the equilibrium (Figure 1B, step −2). The analytical solution of this process is given in Figure 1C, where the signal (S) is defined by changes of the concentration cB.

RESULTS

atToc33, But Not atToc34, Is Regulated by Phosphorylation. The Toc34 isoforms are proposed to belong to a septin-like GTPase family (*23*). However, to establish GTPase function of the homologues proteins of *A. thaliana*, an in vitro assay using purified atToc34ΔTM and atToc33ΔTM was established. Both proteins hydrolyze GTP at a slow rate (Figure 2A, lanes 4 and 5) in a magnesium dependent manner (Figure 2A, lanes 2 and 3). Next, we tested if both atToc34 and atToc33 can be phosphorylated, which inhibits GTP binding (*16*−*18*). To our surprise, only atToc33ΔTM but not atToc34ΔTM (Figure 2B, lanes 2 and 3) was phosphorylated by a kinase present in the outer envelope of chloroplast of *A. thaliana*. The same was observed using outer envelope membranes from *P. sativum* (Figure 2B, lanes 5 and 6) or a kinase purified from wheat germ (ref *16*, data not shown). To investigate if phosphorylation causes an inhibition of GTP binding, atToc33ΔTM was phosphorylated using the outer envelope membranes of *A. thaliana* and incubated with a GDP- or GTP-agarose affinity matrix (Figure 2C). Only the nonphosphorylated subpopulation of atToc33ΔTM was able to interact with both GTP and GDP as determined by antibody decoration (Figure 2C, lanes 3

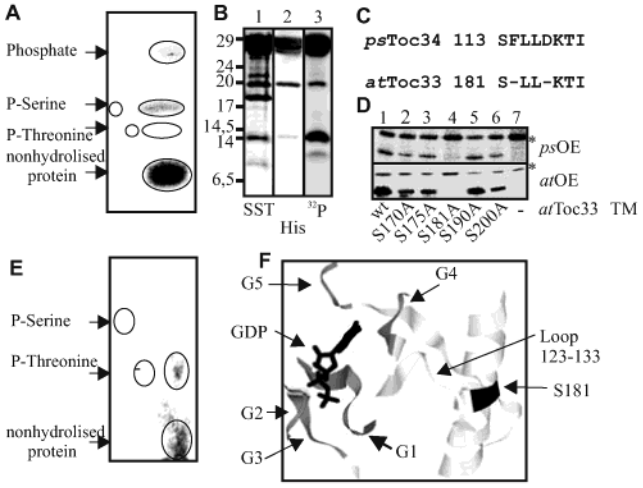

FIGURE 3: AtToc33 is phosphorylated on serine 181. (A) Heterologously expressed atToc33ΔTM was phosphorylated by outer envelopes of *A. thaliana* in the presence of [γ-^{32}P] ATP. The protein was repurified, hydrolyzed, and subjected to PEI cellulose. Positions of the nonlabeled phospho-serine and phospho-threonine standards are indicated. (B) Phosphorylated atToc33ΔTM was digested using V8, and fragments were subjected to SDS−PAGE followed by silver staining (lane 1), immunodecoration using anti-hexa-histidine antibodies (lane 2), or autoradiography (lane 3). (C) A conserved phosphorylation motif is found in *P. sativum* Toc34 and *A. thaliana* Toc33. (D) AtToc33ΔTM (lane 1) harboring a serine to alanine exchange on position 170 (lane 2), 175 (lane 3), 181 (lane 4), 190 (lane 5), and 200 (lane 6) was phosphorylated by outer envelopes of *P. sativum* (upper panel) or *A. thaliana* (lower panel) in the presence of [γ-^{32}P] ATP. Endogenous psToc34 and atToc33 is indicated (*). (E) AtToc33ΔTM/S181T was phosphorylated by outer envelopes of *A. thaliana* in the presence of [γ-^{32}P] ATP. The protein was repurified, hydrolyzed, and subjected to PEI cellulose. Positions of the nonlabeled phospho-serine and phospho-threonine standards are indicated. (F) A model of the GTP binding domains and the location of the phosphorylation site are shown.

and 5, upper panel) and autoradiography (Figure 2C, lanes 3 and 5, lower panel). Therefore, phosphorylation seems to inhibit nucleoside phosphate binding. Subsequently, the interaction of atToc33ΔTM to the small subunit of ribulose 1,5-bisphosphate carboxylase-oxygenase (rubisco; SSU) was investigated using the mature (mSSU, Figure 2D, lanes 4 and5) and precursor form (preSSU, Figure 1D, lanes 6 and 7) coupled to Toyopearl material (Figure 2D, lanes 2 and 3). We observed a specific interaction of atToc33ΔTM only with preSSU but not with mSSU (Figure 2D, compare lanes 5 and 7, upper panel) and exclusively with the nonphosphorylated form of the receptor (Figure 2D, compare lanes 6 and 7, lower panel). We conclude that phosphorylation of atToc33 inhibits its GTP and preprotein binding capacity and further, atToc33 and atToc34 are differentially regulated.

Phosphorylation Site of atToc33. The phosphorylation site of psToc34 is located in the switch 1 region of the GTPase domain at serine 113 (*17*). Interestingly, the alignment between psToc34 and atToc33 revealed that at the same position atToc33 contains a glycine. However, we could confirm that atToc33 is phosphorylated at a serine residue like its homologue in *P. sativum* (Figure 3A). To identify the phospho-amino acid position, the phosphorylated protein was proteolytically digested using the protease V8 (*16*). When the proteolytic fragments where subjected to SDS−PAGE, several peptides could be visualized (Figure 3B, lane 1). A peptide at around 14 kDa was both phosphorylated

(Figure 3B, lane 3) and still contained the carboxy-terminal hexa-histidine tag, as shown by immunoblotting (Figure 3B, lane 2). This indicated that phosphorylation occurred in the C-terminal half of the receptor. The first putative serine within this C-terminal 14 kDa peptide was at position 164. Since this serine is also present in psToc34, we did not expect it to be phosphorylated in atToc33. In contrast, serines 170, 175, 181, 190, and 200 were found to be unique in atToc33. While analyzing the sequence, we identified a similar amino acid motif in atToc33 as in psToc34, which contains the phosphorylated serine 113 (Figure 3C). Even though serine 181 seemed the most likely candidate, we substituted each unique serine with alanine. The proteins harboring the point mutations were phosphorylated (Figure 3D) using outer envelope membranes of chloroplasts from *A. thaliana* (Figure 3D, lower panel) and *P. sativum* (Figure 3D, upper panel). The only protein not phosphorylated was atToc33ΔTMS181A (Figure 3D, lane 4). To confirm that serine 181 is the only phosphorylation site in atToc33, we replaced it by threonine since this amino acid should also be recognized by a serine/threonine kinase. Phosphorylation of Toc33ΔTMS181T was initiated by addition of outer envelope membranes from *A. thaliana*. We observed that this protein is now exclusively phosphorylated at a threonine residue (Figure 3E) confirming that atToc33 is phosphorylated at position 181.

GTP Binding and Hydrolysis Properties of atToc34 and atToc33. Both atToc34 and atToc34 are able to hydrolyze GTP (Figure 2A). To investigate the characteristics of GTP binding, we utilized an IAsys Biosensor. This biosensor uses a dual chamber cuvette and a resonance mirror technique to monitor macromolecular interactions in real time (*21*). His-tagged atToc34ΔTM or atToc33ΔTM was immobilized to an NTA-Ni^{2+} modified carboxymethylated dextran coated cuvette as described in the Materials and Methods. Then, 1 mM GTP or GDP was added to the cuvette to determine the kinetics of the nucleotide binding to the receptor proteins (Figure 4A). No drastic differences between atToc34 and atToc33 could be observed (Figure 4A, Table 1). For both proteins, GTP bound much more rapidly and to a higher extent than GDP (Figure 4A). The association rates (k_{on}) of GTP and GDP differ by a factor larger than three. When the hydrolysis of GTP by atToc33 and atToc34 was analyzed in more detail, we observed an almost similar maximal hydrolysis rate (V_{max}) (Figure 4B). Both proteins revealed a very slow maximal hydrolysis rate of about 500 nM min^{-1} (Table 1). This rate is comparable to the intrinsic GTP hydrolysis rate of other small GTPases (i.e., see refs *30*−*32*). The analysis further revealed a Michaelis−Menten constant of 290 and 190 μM for atToc33 and atToc34, respectively (Table 1). The catalytic constant (k_{cat}) of about 0.3 min^{-1} (Table 1) is comparable to the intrinsic catalytic constant found for other GTPases (i.e., see ref *33*). However, a turnover of one GTP molecule by one receptor every 3 min cannot explain the much more rapid rate of protein translocation into chloroplasts (*34*, *35*). We conclude that both Toc33 and Toc34 can act as a GTPase in vivo but that proteinaceous effectors most likely stimulate their rate of hydrolysis.

Dimerization of atToc33 and atToc34. A homodimer between two receptor molecules was proposed as a functional unit (*27*) as a consequence of the close contact of two of the three psToc34 molecules found in the crystallographic unit.

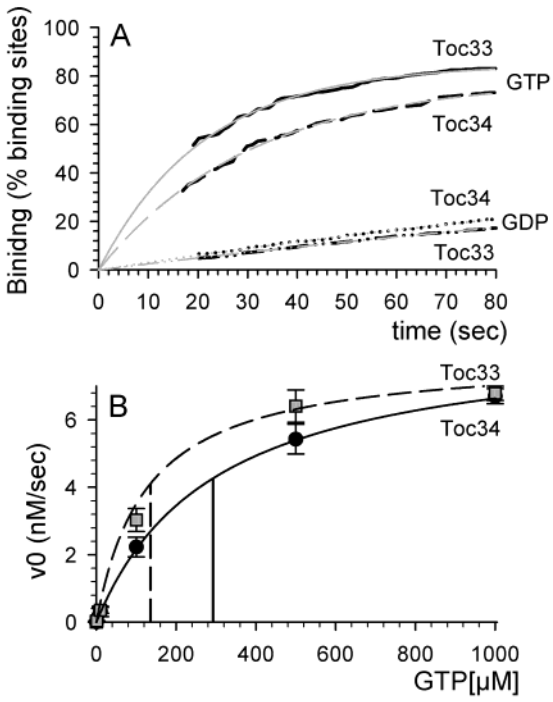

FIGURE 4: GTP binding and hydrolysis properties of atToc33 and atToc34. (A) atToc34ΔTM (dashed and dotted line) and atToc33Δ*T*M (solid and dashed−dotted line) were coupled to an IAsys cuvette to a final concentration of 5 nM and incubated with 1 mM GTP (solid and dashed line) or 1 mM GDP (dotted and dashed−dotted line). The association curve was determined using the IAsys biosensor as described in the Materials and Methods and described in figure legends 5 and 6. The binding was normalized to possible binding by assumption of a single binding site. Black lines represent experimental traces of the binding, and gray lines represent the least-squares analysis using a hyperbolic function according to eq 2. (B) The initial rate constants for different amounts of GTP using 0.5 μg of each protein were determined using [α^{32}P]-GTP as described in the Materials and Methods. Drop lines show the half-maximum giving the K_m value listed in Table 1. Data represent the average of at least four independent measurements, and error bars indicate standard deviation.

Table 1: GTP Binding Rate Constants and Hydrolysis Constants

parameter		Toc33	Toc34
GTP binding[a]	k_{on} (sec^{-1})	0.045 ± 0.003	0.041 ± 0.002
GDP binding[a]	k_{on} (sec^{-1})	0.012 ± 0.004	0.013 ± 0.003
GTP hydrolysis[b]	V_{max} (nM/min)	520 ± 30	470 ± 20
	K_m (M)	(2.9 ± 0.2) × 10^{-4}	(1.3 ± 0.3) × 10^{-4}
	k_{cat} (min^{-1})	0.31 ± 0.01	0.27 ± 0.01

[a] IAsys measurement as described in Figure 4A. [b] Experiment described in Figure 4B.

Furthermore, it was observed that Toc34 interacts with the highly homologous GTPase domain of Toc159 (*36*). Here, we wanted to study the nature of such dimerization. The interaction of atToc33 and atToc34 was investigated in the absence (Figure 5A) or presence of nucleotides (Figure 5B,C). In the presence of GDP or without any nucleotides, the highest binding efficiency was observed for atToc34−atToc33 interaction (Figure 5A,B, solid line). In the presence of GTP, the association between Toc34 and Toc33 was in the range of the homodimerization between Toc33 and Toc33 or Toc34 and Toc34, respectively. Homodimerization seemed to be less dependent on the presence of nucleotides (Figure

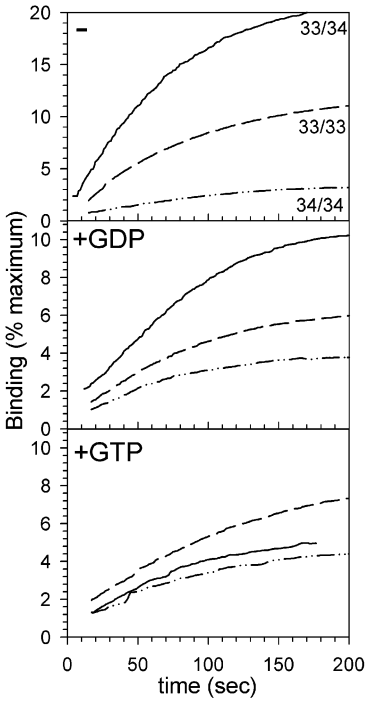

FIGURE 5: Homo- and heterodimerization of atToc33 and atToc34. The association between atToc33ΔTM and atToc34ΔTM was investigated by utilizing an optical biosensor instrument (IAsys). The raw data expressed in arcsec to reflect the increase of the density on the cuvette surface were calibrated for the maximal amount of possible binding assuming a single binding site (maximal binding, related to the amount of receptor coupled) and data expressed as percent of the maximum. A representative binding curve is shown. In detail, 7 ng of atToc33ΔTM (dashed line) and atToc34ΔTM (dashed−dotted and solid lines) were coupled to the dextran surface as described in the Materials and Methods followed by incubation with 175 ng of atToc33ΔTM (dashed and solid lines) and atToc34ΔTM (dashed−dotted line) in the absence of nucleotides (upper panel, −), in the presence of 1 mM GDP and 1 mM $MgCl_2$ (middle panel, +GDP) or in the presence of 1 mM GTP and 1 mM $MgCl_2$ (lower panel, +GTP).

Table 2: Dissociation Constants and Dissociation Rate Constants for Receptor Dimerization[a]

nucleotide	constant	Toc33/Toc33	Toc34/Toc34	Toc33/Toc34
GTP	K_d (nM)[b]	720 ± 60	1530 ± 180	1020 ± 90
	k_{diss} (sec^{-1})	0.0025 ± 0.0006	0.007 ± 0.003	0.002 ± 0.001
GDP	K_d (nM)	830 ± 70	2100 ± 200	370 ± 30
	k_{diss} (sec^{-1})	0.02 ± 0.01	0.05 ± 0.003	0.06 ± 0.03
No	K_d (nM)	490 ± 30	1670 ± 130	200 ± 30
	k_{diss} (sec^{-1})	0.006 ± 0.004	0.004 ± 0.001	0.004 ± 0.002

[a] For description, see Figure 5 legend. [b] Calculated using $K_d = 100\% \times conc/R_{max} - conc$ (*21*).

5A−C). The association efficiency is also reflected by the dissociation constant (K_d, Table 2). Remarkably, the lowest dissociation constant (K_d) of approximately 200 nM was observed for the heterodimer in the absence of nucleotides. The homodimer of atToc33, but not of atToc34, also revealed a low dissociation constant in the absence of nucleotides (K_d, Table 2). Under all conditions, the homodimer of atToc34 revealed the highest dissociation constant (K_d, Table 2). These results suggest that dimerization of atToc33 and atToc34 is unfavorable in the presence of GTP. In addition, heterodimerization is preferred in comparison to homodimerization. Taking into account that the G-domain of Toc159 is very homologous to the Toc34/33 G domain (*4*, *5*), our result supports the idea from Hiltbrunner and co-workers (*36*) that heterodimerization of the G-domains of the Toc receptor components might be important for the assembly and function of the Toc complex (*22*, *37*).

A more detailed analysis of the association between the receptor proteins revealed the highest dissociation rate (k_{diss}) for the heterodimer in the presence of GDP. In contrast, the dissociation rates (k_{diss}) in the presence of GTP or in the absence of nucleotides are comparable. This finding, together with the observation that the dissociation constant (K_d) for the heterodimer is highest in the presence of GTP (Table 2), reveals that the association rate constant (k_{ass}) is lowest in the presence of GTP. This result directly contradicts the hypothesis that dimerization acts as a GTPase activating protein factor (GAP) (*27*). A GAP typically reveals the highest association rate constant and the lowest dissociation constant for its substrate in the presence of GTP (*38*). In contrast, the heterodimer reveals a high dissociation rate constant (k_{diss}) but the rather low dissociation constant (K_d, Table 2) suggesting a rather high association rate constant in the presence of GDP. This leads to the speculation that this interaction might instead act as a GEF (GDP/GTP exchange factor) (*39*). This could also explain the results that abolishment of the interaction between the two GTPase domains leads to a reduction of the intrinsic GTPase activity (*27*).

Preprotein Binding of atToc34 and atToc33. AtToc33 and atToc34 are both GTPase type receptor proteins for chloroplast-targeted preproteins. We therefore investigated the interaction of different preproteins from *A. thaliana* with the two receptor proteins. We observed typical binding traces for the interaction of atToc33 and atToc34 to the precursor of Ferredoxin:$NADP^+$ oxidoreductase (FNR) in the absence of GTP (Figure 6A). In contrast, when GTP was present, a new type of binding trace was found for the association between atToc34 and atToc33 and different precursors (FNR is shown as example in Figure 6B,C). After an initial rapid association the signal decreased (Figure 6B,C). Finally, a second association could be observed (Figure 6B,C). In some cases, the association was too rapid to observe the initial increase of the signal since stirring and mixing effects do not allow the analysis of the first 5−10 s. Therefore, we developed a model to analyze these data further.

Taking the existing knowledge about the behavior of Toc34 from *P. sativum* into account, this curve can be explained by the following. The initial GTP preloaded Toc34 has a very high affinity for preproteins (*16*, *21*). This association stimulates GTP hydrolysis and dissociation of the preprotein (*17*). Since GTP exists in excess, GDP to GTP exchange occurs because atToc33/34 binds GTP with higher affinity than GDP (Figure 4, Table 2). Finally, equilibrium between precursor association and dissociation will be observed. Furthermore, when we repeated the binding experiment in the presence of the non-hydrolysable GTP analogue, GMP-PNP, such a three-phase behavior was not observed (Figure 6D). In Figure 1A, the mathematical solution of the reaction is outlined; however, such a model cannot be described analytically. Therefore, we used a three-phase model as described in Figure 1B to extrapolate values from this binding tray. To confirm the assumption that we truly detect the GTPase activity of atToc33/34 and its

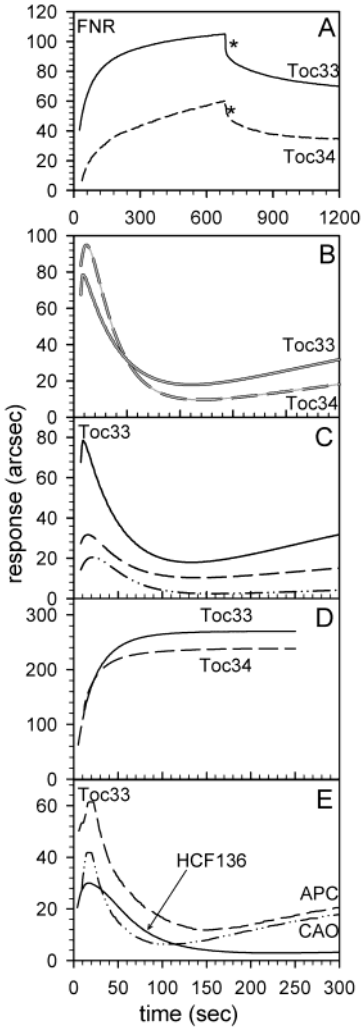

FIGURE 6: Nucleotide dependent binding of preproteins by at Toc33 and atToc34. The association (A−D) and dissociation (A) between both receptor proteins and FNR was investigated using an optical biosensor instrument (IAsys). The increase/decrease of the density on the cuvette surface reflecting the increase/decrease of formed complexes is represented in arbitrary units and presented as response in arcsec. Representative binding traces are shown. In panel A, 5 ng of atToc33ΔTM (solid line) and atToc34ΔTM (dashed line) were coupled to the dextran surface and incubated with 440nM FNR in the absence of GTP. After the indicated time (*), dissociation was initiated by removal of the free FNR. In panel B, 7 ng of atToc33ΔTM (solid line) and atToc34ΔTM (dashed line) were coupled to the IAsys chamber and incubated with 16 nM FNR in the presence of 1 mM GTP and 1 mM $MgCl_2$. In panel C, 7 ng of atToc34ΔTM were incubated with 7.9 nM (dotted line), 10.9 nM (dashed line), or 16 nM FNR (solid line) in the presence of 1 mM GTP and 1 mM $MgCl_2$. (D) 7 ng of atToc33ΔTM (solid line) and atToc34ΔTM (dashed line) were coupled to the IAsys chamber and incubated with 16 nM FNR in the presence of 1 mM GMP-PNP and 1 mM $MgCl_2$. (E) 7 ng of atToc33ΔTM was coupled to the IAsys chamber and incubated with 23 nM HCF136 (solid line), 42.4 nM APC (dashed line), or 36.3 nM CAO (dashed−dotted line) in the presence of 1 mM GTP and 1 mM $MgCl_2$.

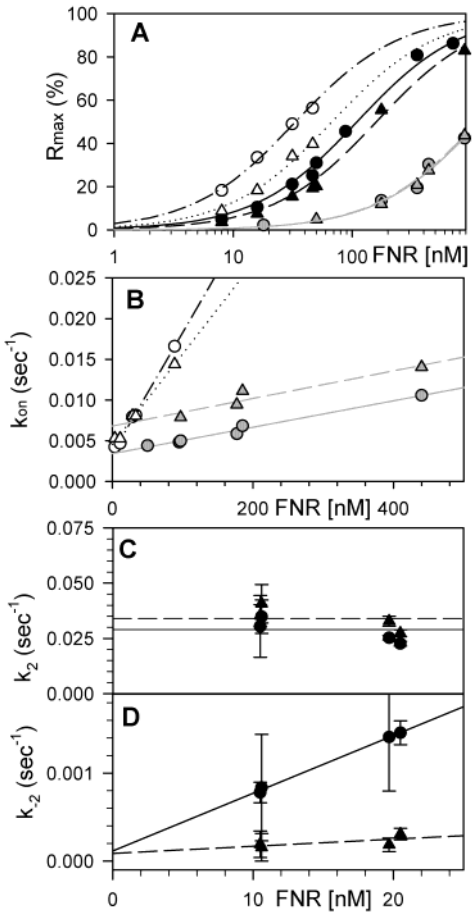

FIGURE 7: Binding properties of preFNR to atToc33 and atToc34. As described in the legend of Figure 6, the receptor proteins were coupled to the cuvette surface, and association and dissociation between both proteins was determined. The binding traces were analyzed as described in the Materials and Methods and the references therein. All data points (A−D) reflect the average of at least four independent measurements. In panel A, 7 ng of atToc33ΔTM (solid and dashed−dotted line, circle) and atToc34ΔTM (dashed and dotted line, triangle) were coupled to the dextran surface and incubated with the indicated amounts of preFNR in the absence of nucleotides (gray symbols and lines), in the presence of 1 mM GTP and 1 mM $MgCl_2$ (black symbols and solid or dashed line), or in the presence of 1 mM GMP-PNP and 1 mM $MgCl_2$ (open symbols and dashed−dotted or dotted line). The final amount of bound protein is shown observed at equilibrium of the association (R_{max}) normalized for the amount of binding sites assuming a single binding site on the receptor. Lines represent least-squares analysis of the data points to a hyperbolic curve for dissociation constant determination. In panel B, the on-rates for the association in the absence or presence of GMP-PNP are plotted against the concentration precursor used to determine the association constant k_{ass}. Symbols and colors of gray are according to panel A. Lines represent the linear regression. (C and D) The rate constant 2 (C) and −2 (D) (according to Figure 1B) are plotted against the concentration of FNR used in the experiment. Symbols and colors of gray are according to panel A. Lines represent the linear regression.

stimulation by incoming preproteins, samples were taken out of the cuvette and spotted onto PEI-cellulose plates. We observed increasing amounts of GDP over time (not shown).

When the association of preFNR was analyzed, we determined a high dissociation constant (K_d) in the absence of GTP for both atToc33 and atToc34 (Figure 7A, gray symbols, Table 3). In the presence of GMP-PNP, the affinity between FNR and atToc33/34 was drastically increased (Figure 7A, open symbols, Table 3). The observed dissociation constants (K_d) are 30-fold lower than in the absence of the nucleotide (Table 3). We conclude that both receptor proteins recognize the incoming preprotein with highest affinity in the GTP bound state. The analysis of the amount of binding at equilibrium in the presence of GTP according to the three-phase binding model (Figure 1B) revealed a

Table 3: Dissociation Constants and Rate Constants for Preprotein Recognition

preprotein	nucleotide	parameter	Toc33	Toc34
FNR[a]	no	K_d (nM)	1170 ± 30 (460)	1140 ± 30 (1140)
		k_{diss} (sec^{-1})	0.0068 ± 0.0002	0.0182 ± 0.0002
		k_{ass} ($M^{-1}\,sec^{-1}$)	(1.7 ± 0.4) × 10^4	(1.6 ± 0.4) × 10^4
FNR[a]	GTP	K_d (nM)	110 ± 10	160 ± 20
		k_2 (sec^{-1})	0.028 ± 0.004	0.034 ± 0.003
		k_3 ($M^{-1}\,sec^{-1}$)	(6.6 ± 0.3) × 10^4	(8.1 ± 0.7) × 10^3
FNR[a]	GMP-PNP	K_d (nM)	3 3± 1	68 ± 2
		k_{ass} ($M^{-1}\,sec^{-1}$)	(1.5 ± 0.4) × 10^5	(1.1 ± 0.4) × 10^5
APC[a]	GTP	K_d (nM)	210 ± 20	46 ± 1
		k_2 (sec^{-1})	0.027 ± 0.001	0.042 ± 0.005
		k_3 ($M^{-1}\,sec^{-1}$)	(2 ± 1) × 10^4	(6 ± 2) × 10^4
	GMP-PNP	K_d (nM)	199 ± 10	22.2 ± 0.5
		k_{ass} ($M^{-1}\,sec^{-1}$)	(9.0 ± 0.5) × 10^4	(1.0 ± 0.3) × 10^6
HCF136[a]	GTP	K_d (nM)	158 ± 9	220 ± 10
		k_2 (sec^{-1})	0.030 ± 0.003	0.040 ± 0.008
		k_3 ($M^{-1}\,sec^{-1}$)	(5.6 ± 0.8) × 10^3	(2.8 ± 0.6) × 10^4
CAO[a]	GTP	K_d (nM)	270 ± 30	102 ± 8
		k_2 (sec^{-1})	0.024 ± 0.004	0.035 ± 0.006
		k_3 ($M^{-1}\,sec^{-1}$)	(2.9 ± 0.3) × 10^4	(2.6 ± 0.6) × 10^5

[a] IAsys measurement as described in Figures 6 and 7.

3-fold higher dissociation constant (K_d) than in the presence of GMP-PNP. This is in line with the assumption that this state reflects the equilibrium between bound and unbound precursor. Furthermore, the association of preFNR with atToc33 was found to be of higher affinity than the association with atToc34 (Figure 7A, Table 3). As expected, the difference of the dissociation constants in the absence or presence of nucleotides is due to a drastic alteration of the association rate constant (k_{ass}) by a factor of 10 (Figure 7B, Table 3). Analysis of the three-phase reaction in the presence of GTP revealed a second rate constant (k_2) of 0.028 and 0.034 s^{-1} for atToc33 and atToc34, respectively (Table 2). This rate constant (k_2) is not dependent on the concentration of the ligand (Figure 7C) since the reaction described is a dissociation type process (Figure 1B). This further suggests that the dissociation of preFNR from the receptor is almost comparable between atToc33 and atToc34. The third rate constant (k_{-2}) is again concentration dependent (Figure 7D) since association is involved in the process covered by the last step (Figure 1B). It is found that the association between atToc33 and preFNR reaches the equilibrium faster than found for atToc34/preFNR (Figure 7D) being in line with atToc33 having a higher affinity for preFNR as compared to atToc34.

Since we observed different binding affinities of atToc33 and atToc34 for FNR (Table 3), we asked whether this could be seen for other preproteins as well. We subsequently investigated the association of three further preproteins to atToc33 and atToc34, namely, preAPC (Figure 6E), the precursor of the high chlorophyll fluorescence protein 136 (preHCF136, Figure 6E) and the precursor form of the chlorophyll *a* oxygenase (preCAO, Figure 6E). The association of all four preproteins in the presence of GTP revealed a three-phase behavior. However, we observed that preHCF136 has a slightly higher affinity and a lower dissociation constant (K_d), respectively, for atToc33 when compared to atToc34. In contrast, atToc34 has a significantly lower dissociation constant (K_d) as compared to atToc33 when bound to preAPC or preCAO (Table 3).

A closer look at the second rate constant (k_2) suggested that the dissociation is higher in the presence of GDP than in the absence of any nucleotide (for preFNR), but comparable for all preprotein receptor combinations. This supports the hypothesis that the GDP bound state does not recognize any preproteins since otherwise strong variations of this rate constant would have been expected. The third association rate is related to the association rate as seen for preAPC and preFNR suggesting that the proposed model (Figure 1B) can be used to describe the observed binding behavior. However, the GTP binding seems not to be the rate-limiting step since otherwise the same rate constants for all preproteins would have been expected.

We suggest that atToc33 has a higher affinity for preFNR and preHCF136, whereas atToc34 revealed a higher affinity for preAPC and preCAO.

Stimulation of GTP Hydrolysis by atToc33 and atToc34 Is Substrate Dependent. AtToc34 and atToc33 are both GTPases (Figure 2) recognizing different subsets of preproteins (Figures 6 and 7; Table 3). Furthermore, the intrinsic hydrolysis rate (Figure 4 and Table 1) suggests a stimulation of the hydrolysis by a GAP component. The first hypothesis that homodimerization might cause such stimulation (*27*) could not be confirmed for two reasons. First, homo- or heterodimerization reveals the highest affinity in the absence of nucleotides (Figure 5, Table 2). Second, all hydrolysis experiments so far were performed in solutions allowing dimerization. However, a second hypothesis suggested that incoming preproteins might function as GTPase stimulating factors (*17*). To test this hypothesis and to demonstrate that hydrolysis of GTP to GDP causes release of the preprotein, atToc33 was preincubated with GTP reisolated and subsequently incubated with preSSU. The amount of hydrolyzed GTP and released preSSU was quantified at different time points (Figure 8A). It can be clearly demonstrated that the amount of hydrolysis correlates almost in a 1:1 ratio with the amount of released preSSU (Figure 8A, circle). In comparison, almost no preSSU was released in the presence of GMP-PNP (Figure 8A, open square).

Therefore, we conclude that the hydrolysis of 1 mol of GTP results in the release of 1 mol of preprotein from the receptor atToc33.

Next, we asked if the differential affinities of the two receptor proteins for preproteins are also reflected in the potential to differentially stimulate the GTPase activity of atToc33 and atToc34. We tested the effect of six preproteins, namely, preFNR, preAPC, preHCF136, preCAO (from *A. thaliana*), and the precursor forms of the 23 and 33 kDa subunits of the oxygen evolving complex preOE23 and preOE33 (*P. sativum*). Strikingly, a stimulation of hydrolysis was observed in all cases. However, as seen for the association, the extent of activation was dependent on the receptor−preprotein combination. In line with the binding behavior, preFNR stimulated atToc33 GTP hydrolysis 28-fold. Furthermore, preOE23, preOE33, and preHCF136 were also found to stimulate the GTP hydrolysis of atToc33 more pronounced than GTP hydrolysis by atToc34. In contrast, preAPC stimulated the GTP hydrolysis of atToc34 by a factor of 32 but only 14-fold that of atToc33 (Figure 8B). However, in line with the observed dissociation constants, the stimulation by preHCF136 and preCAO was not as pronounced as found for the other precursor proteins. Therefore, preprotein recognition seems to initiate GTPase activation.

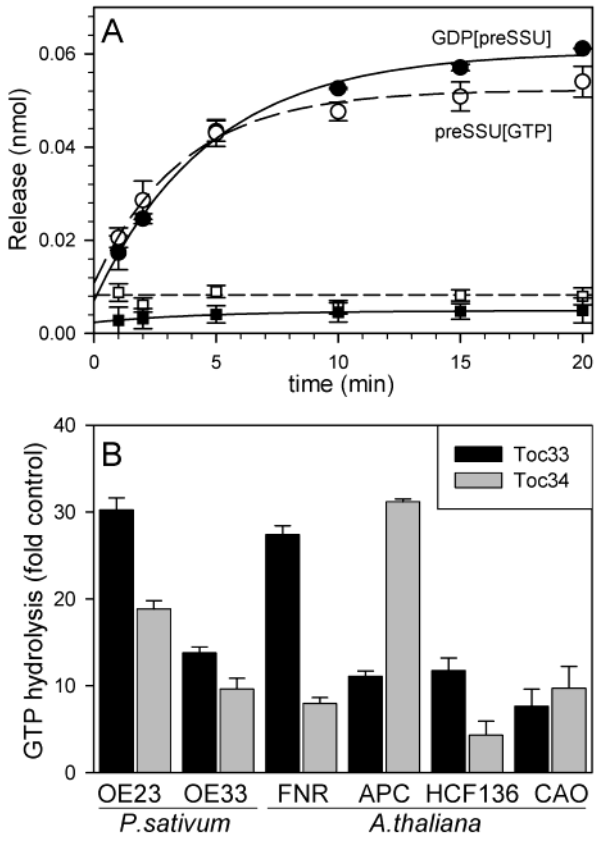

FIGURE 8: Differential stimulation of atToc33 and atToc34 GTP hydrolysis by recognition of preproteins. (A) 0.1 nmol of Toc33 was loaded with GTP and preSSU as described in the Materials and Methods. The molar amount of released phosphate after hydrolysis of GTP in the presence (closed circle) or absence of preSSU (closed squares) and released preSSU in the presence of GTP (open circle) or GMP-PNP (open squares) at indicated time-points are shown. Each data point is the average of at least two independent experiments. Lines represent least-squares analysis to a monophasic kinetic. (B) The hydrolysis of the GTP by 0.1 μg of Toc34 and Toc33 proteins in the presence of 20-fold molar excess of the indicated preprotein was determined. The fold of hydrolysis increase as compared to hydrolysis in the absence of preprotein is shown. Error bars indicate the standard deviation of at least four independent experiments.

DISCUSSION

The Toc34 isoforms belong to the P-loop type GTPase subfamily of septin like proteins (*23*). We demonstrated that both atToc33 and atToc34 are able to bind (Figure 4A) and hydrolyze GTP (Figures 2A and 4B). Interestingly, only atToc33 is phosphorylated. Phosphorylation occurs at the position of serine 181 (Figure 3) at a conserved amino acid motif (Figure 3C), which can also be found in Toc34 of *O. sativa* (*40*) and *P. sativum* (*6*, *7*). Phosphorylation inhibits GTP binding and hence precursor recognition (Figure 2C,D). In the case of psToc34, the influence of phosphorylation on GTP binding was easier to visualize since phosphorylation occurs within the essential switch 1 domain (*17*). Phosphorylation in atToc33 occurs closer toward the C-terminus. However, as indicated in Figure 3F, phosphorylation of serine 181 would disturb the general organization of the GTP-binding domain. First, a structural deformation of the long helix might result in the deformation of G5. Another explanation might be that the incorporation of the phosphate strongly interferes with the highly charged loop between amino acids 123 and 133. This loop, however, interacts with the G4 and G1 region. Therefore, three of the five important domains recognizing GTP might be affected by the phosphorylation of serine 181, explaining the interference with the GTP binding ability of atToc33.

GTP binding of a single receptor molecule (Figure 4A, Table 1) as well as the turnover rate of the intrinsic hydrolysis of GTP (Figure 4B, Table 1) was found to be rather slow but similar for both receptors. The catalytic constant of about 0.3 min^{-1} (Table 1) representing a turnover of one GTP molecule by one receptor every 3 min would be unable to support the rapid protein translocation observed into chloroplasts. For example, it was observed that about 20 000 ferredoxin molecules per minute per chloroplast can be imported (*34*, *35*). Taking into account that only 10% of the about 20 000 protein translocation complexes (*41*) are active (*42*), we must expect a stimulation of GTP hydrolysis by the receptors by further components.

For example, it was proposed that homodimerization might result in such stimulation. To our surprise, the highest affinity of dimerization was found in the absence of nucleotides (Figure 5, Table 2). Even further, the presence of nucleotides drastically reduces the affinity for homodimerization (Figure 5, Table 2). This observation contradicts the hypothesis that homodimerization functions as GAP. Furthermore, GAPs have the highest affinity for the GTPase in the presence of GTP (*38*, *43*), which was not found in this study. Interestingly, the affinity of the heterodimeric complex was not significantly different in the presence of GDP or in the absence of nucleotides. This supports the idea of a hetero-oligomerization of atToc34 or atToc33 with other G-domain containing Toc components such as atToc159, atToc132, atToc120, or atToc90 (*36*). However, this interaction might lead to a GEF activation of the GTPases by dimerization (*22*, *37*) since GEFs recognize their substrate in the GDP bound form (*39*).

Transit peptides are enriched in arginines, which are supposed to form the catalytic amino acids of the GAPs (*43*). Therefore, preproteins might function as GTPase activating proteins. In support of this hypothesis, we observed an increase of GTP hydrolysis by the receptors up to 30-fold after preprotein recognition (Figure 8). This is in line with the observation that 20 000 preprotein molecules can be inserted into one chloroplast (*34*, *35*) representing 1500−3000 active complexes (*42*) since the turnover would be increased at least to 10 GTP molecules per minute resulting in 15 000−30 000 potential translocation events per minute. In addition, the hypothesis of a GAP function for the preprotein is also in line with the observation that preproteins reveal the highest affinity for atToc33/34 in the presence of GTP (Figure 6, Table 3). The observed dissociation constants in the presence of GMP-PNP of atToc34/33 and preFNR are 30-fold lower than in the absence of the nucleotide (Table 3) and comparable to the dissociation constant found for the interaction between preSSU and psToc34 in the presence of GTP (*21*). Comparison between the off rate, k_2, in the presence of GTP and the dissociation rate constant, k_{diss}, in the absence of nucleotides, reveals a 3-fold increase in the presence of GDP (remembering that dissociation occurs after hydrolysis). This supports the theory that hydrolysis allows the preprotein to move further through the translocation event. In addition, the hydrolysis rate and the rate of the dissociation of a preprotein were found to be similar (Figure 8A). Taken together, the Toc34 proteins act as a GTPase type receptor for preproteins, and hydrolysis is at least regulated by the recognition of the preprotein. The preprotein will be released in the presence of GDP and subsequently translocated. However, the question remains as to why do two isoforms exist if the mode of action is comparable?

Both proteins are differentially expressed (*14*) and differentially regulated (Figure 2). We further identified that both receptors reveal differential affinities for different preproteins. Whereas atToc33 recognized preOE23, preOE33 (data not shown), preFNR, and preHCF136 (Table 3) with higher affinity than atToc34, the later revealed a higher affinity for preAPC and preCAO. The same tendency was subsequently found for the stimulation of the GTP hydrolysis of the receptor proteins by the different preproteins (Figure 8), which is in line with the observation that atToc34 cannot fully complement *A. thaliana* plants with a deletion of atToc33 (*13*). However, the ability of both receptor proteins to recognize all preproteins, even though with different affinity (Table 3, Figure 8), together with the observed dominant localization of atToc34 in roots (*14*) might explain why root plastids in the atToc33 knock out line are able to differentiate into chloroplasts after prolonged light treatment (*15*). The observed phenotype of the deletion of atToc33 might in addition be explained by the differential expression of atToc34 and atToc33 in contrast to an explicit functional difference. Indeed, Jarvis et al. (*13*) found that when atToc34 was expressed earlier in development, it was able to complement the atToc33 null phenotype. This again is in line with the observation that all preproteins are recognized by both receptor proteins even though with different affinity.

The identification of differential regulation of the two receptors as well as the preferential recognition of different preproteins is the first step in understanding the existence of two different isoforms of the Toc34 family. The dissection of the preprotein features resulting in preferential recognition by each receptor, however, remains elusive. Answering this question requires investigation of a larger pool of preproteins since the simple division of photosynthetic and nonphotosynthetic proteins (*11*, *13*) seems oversimplified as even photosynthetic proteins reveal different affinities and stimulation behaviors (Figure 8).

ACKNOWLEDGMENT

We are grateful to Dr. Gutensohn for providing us with the original atToc33 and atToc34, to Prof. Westhoff for preCAO, and to Dr. J. Meurer for preHCF136 and preAPC.

REFERENCES

1. Keegstra, K., and Cline, K. (1999) *Plant Cell 11*, 557−570.
2. Schleiff, E., and Soll, J. (2000) *Planta 211*, 449−456.
3. Kessler, F., and Schnell, D. J. (2002) *Nat. Struct. Biol. 9*, 81−83.
4. Kessler, F., Blobel, G., Patel, H. A., and Schnell, D. J. (1994) *Science 266*, 1035−1039.
5. Hirsch, S., Muckel, E., Heemeyer, F., von Heijne, G., and Soll, J. (1994) *Science 266*, 1989−1992.
6. Seedorf, M., Waegemann, K., and Soll, J. (1995) *Plant J. 7*, 401−411.
7. Schnell, D. J., Kessler, F., and Blobel, G. (1994) *Science 266*, 1007−1012.
8. Tranel, P. J., Froehlich, J., Goyal, A., and Keegstra, K. (1995) *EMBO J. 14*, 2436−2446.
9. Sohrt, K., and Soll, J. (2000) *J. Cell Biol. 148*, 1213−1221.
10. Jackson-Constan, D., and Keegstra, K. (2001) *Plant Physiol. 125*, 1567−1576.
11. Bauer, J., Chen, K., Hiltbunner, A., Wehrli, E., Eugster, M., Schnell, D., and Kessler, F. (2000) *Nature 403*, 203−207.
12. Hiltbrunner, A., Bauer, J., Alvarez-Huerta, M., and Kessler, F. (2001) *Biochem. Cell Biol. 79*, 629−635.
13. Jarvis, P., Chen, L. J., Li, H., Peto, C. A., Fankhauser, C., and Chory, J. (1998) *Science 282*, 100−103.
14. Gutensohn, M., Schulz, B., Nicolay, P., and Flügge, U. I. (2000) *Plant J. 23*, 771−783.
15. Yu, T. S., and Li, H. (2001) *Plant Physiol. 127*, 90−96.
16. Sveshnikova, N., Soll, J., and Schleiff, E. (2000) *Proc. Natl. Acad. Sci. U.S.A. 97*, 4973−4978.
17. Jelic, M., Sveshnikova, N., Motzkus, M., Hörth, P., Soll, J., and Schleiff, E. (2002) *Biol. Chem. 383*, 1875−1883.
18. Soll, J. (1985) *Planta 166*, 394−400.
19. Fulgosi, H., and Soll, J. (2002) *J. Biol. Chem. 277*, 8934−8940.
20. Kouranov, A., and Schnell, D. J. (1997) *J. Cell Biol. 139*, 1677−1685.
21. Schleiff, E., Soll, J., Sveshnikova, N., Tien, R., Wright, S., Dabney-Smith, C., Subramanian, C., and Bruce, B. D. (2002) *Biochemistry 41*, 1934−1946.
22. Smith, M. D., Hiltbrunner, A., Kessler, F., and Schnell, D. J. (2002) *J. Cell Biol. 159*, 833−843.
23. Leipe, D. D., Wolf, Y. I., Koonin, E. V., and Aravind, L. (2002) *J. Mol. Biol. 317*, 41−72.
24. Bourne, H. R., Sanders, D. A., and McCormick, F. (1990) *Nature 348*, 125−132.
25. Bourne, H. R., Sanders, D. A., and McCormick, F. (1991) *Nature 349*, 117−127.
26. Reuber, T. L., and Ausubel, F. M. (1996) *Plant Cell 8*, 241−249.
27. Sun, Y. J., Forouhar, F., Li, H. M., Tu, S. L., Yeh, Y. H., Kao, S., Shr, H. L., Chou, C. C., Chen, C., and Hsiao, C. D. (2002) *Nat. Struct. Biol. 9*, 95−100.
28. Schleiff, E., Motzkus, M., and Soll, J. (2002) *Plant Mol. Biol. 50*, 177−185.
29. Soll, J., Fischer, I., and Keegstra, K. (1988) *Planta 176*, 488−496.
30. Downward, J., Riehl, R., Wu, L., and Weinberg, R. A. (1990) *Proc. Natl. Acad. Sci. U.S.A. 87*, 5998−6002.
31. Zhang, B., Wang, Z. X., and Zheng, Y. (1997) *J. Biol. Chem. 272*, 21999-2007.

32. Albert, S., Will, E., and Gallwitz, D. (1999) *EMBO J. 18*, 5216−5225.
33. Rutthard, H., Banerjee, A., and Makinen, M. W. (2001) *J. Biol. Chem. 276*, 18728−18733.
34. Pilon, M., Weisbeek, P. J., and de Kruijff, B. (1992) *FEBS Lett. 302*, 65−68.
35. van't Hof, R., and de Kruijff, B. (1995) *J. Biol. Chem. 270*, 22368−22373.
36. Hiltbrunner, A., Bauer, J., Vidi, P. A., Infanger, S., Weibel, P., Hohwy, M., and Kessler, F. (2001) *J. Cell Biol. 154*, 309−316.
37. Bauer, J., Hiltbrunner, A., Weibel, P., Vidi, P. A., Alvarez-Huerta, M., Smith, M. D., Schnell, D. J., and Kessler, F. (2002) *J. Cell Biol. 159*, 845−854.
38. Kraemer, A., Brinkmann, T., Plettner, I., Goody, R., and Wittinghofer, A. (2002) *J. Mol. Biol. 324*, 763−774.
39. Cherfils, J., and Chardin, P. (1999) *Trends Biochem. Sci. 24*, 306−311.
40. Hirohashi, T., and Nakai, M. (2000) *Biochim. Biophys. Acta 1491*, 309−314.
41. Morin, X. K., and Soll, J. (1997) *Planta 201*, 119−127.
42. Friedman, A. L., and Keegstra, K. (1989) *Plant. Phys. 89*, 993−999.
43. Vetter, I. R., and Wittinghofer, A. (2001) *Science 294*, 1299−1304.

BI034001Q